Improved UAV Path Planning in Urban Environment Based on A-Star Method

Jiaqi Song[1]*and Rongjun Zhou[2]

[1]Leeds Joint School, Southwest Jiaotong University, Sichuan Province, 611756, China
[2] School of Mechanical and Materials Engineering, North China University of Technology, Beijing, 100144, China
*mn22js2@leeds.ac.uk

Abstract. With the development of technology, unmanned aerial vehicles (UAVs) are increasingly utilized in civil applications. Several provinces and cities in China are vigorously developing the low-altitude economy, with industrial environments gradually maturing. However, traditional A-star algorithms produce complex results in UAV applications, potentially leading to collision risks and energy waste. This study aims to enhance the A-star algorithm to address UAV autonomous flight challenges in complex environments, prevent collisions, expand application scenarios, and reduce costs through shorter path distances. By analyzing urban environments and obstacle-dense areas, improvements are made to the path planning algorithm based on an optimized A-star framework. Specifically, dynamic local path adjustments via the Artificial Potential Field (APF) method are integrated into the globally optimal paths generated by the A-star algorithm. Algorithm performance is evaluated and compared, including pre- and post-improvement data analysis, assessment metrics, and result interpretation. Validation confirms that the improved algorithm reduces path length by approximately 8% compared to the original A-star, while the shortest distance between obstacles increases by around 50%. These findings provide theoretical and technical support for efficient UAV applications in urban environments.

Keywords: UAV; Urban Environment; Path Planning; Control Staategies

1 Introduction

The development of UAV path planning algorithms has been diverse, evolving from early graph-search methods (e.g., A-star, Dijkstra) to more flexible heuristic search algorithms, and further to probabilistic path planning methods (e.g., Probabilistic Roadmap (PRM), Rapidly-exploring Rand Tree (RRT), and variants like RRT* and Informed RRT*) [1-3]. Bionic intelligent algorithms are also applied to path planning. In recent years, machine learning and deep learning techniques have been widely applied to UAV path planning, enabling UAVs to learn planning strategies from sensor data and adapt to complex environments. Additionally, multi-agent collaborative planning, high-precision maps, and sensor fusion technologies have advanced UAV

J. Iqbal (ed.), *Proceedings of the 2025 2nd International Conference on Mechanics, Electronics Engineering and Automation (ICMEEA 2025)*, Advances in Engineering Research 272,
https://doi.org/10.2991/978-94-6463-821-9_110

path planning, improving coordination efficiency in multi-UAV systems and path planning accuracy [4].

Common path planning algorithms include search-based, probabilistic, and intelligent algorithm-based methods. Search-based algorithms (e.g., A-star, Dijkstra) can identify globally optimal paths but face challenges in 3D environments due to the complexity and high computational cost of constructing grid maps. Probabilistic algorithms (e.g., PRM, RRT, RRT*) eliminate grid map requirements, making them suitable for high-dimensional environments. They offer probabilistic completeness and low computational load but suffer from inconsistent paths due to random sampling, lack of optimality guarantees, and slower planning speeds. Intelligent algorithm-based methods (e.g., genetic algorithms, ant colony algorithms) exhibit strong global search capabilities for complex environments but struggle with poor generalization, parameter tuning difficulties, and high computational costs [5].

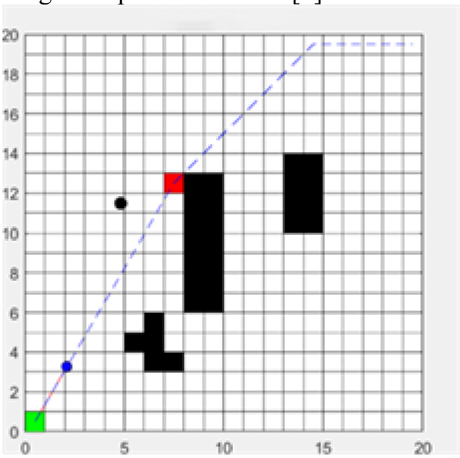

Fig. 1. Grid Example Diagram

This study focuses on optimizing the traditional A-star algorithm using the Artificial Potential Field (APF) method. The goal is to enable UAVs to avoid dynamic obstacles, refine safety distance assessments between UAVs and obstacles, and enable timely local path adjustments. Theoretically, the optimized algorithm enhances path safety in specific scenarios compared to conventional A-star algorithms, reducing collision risks. Although path lengths may increase slightly, accident risks are effectively mitigated. Moreover, when the original A-star path already maintains a safe distance from obstacles, the optimized algorithm avoids unnecessary modifications to prevent adverse effects. These improvements expand UAV application potential in urban logistics, surveillance, and other domains, significantly advancing UAV deployment in urban environments [6].

The remainder of this paper is organized as follows: Section 2 analyzes urban environmental characteristics, outlines the algorithm improvement framework, and describes simulation experiments for validation. Section 3 presents simulation results and verifies the algorithm's enhancements. Section 4 summarizes the improvements and discusses future research directions.

2 Methodology

2.1 Characteristics of Urban Environments and Obstacle-Dense Areas

Urban environments are densely populated with obstacles such as buildings and pedestrian/vehicle traffic, resulting in more complex spatial distributions compared to open areas, with numerous mobile obstacles (e.g., pedestrians, vehicles). Additionally, urban settings impose no-fly zones on UAVs. To scientifically plan delivery paths for logistics UAVs, urban 3D flight environment modeling is essential. Common environment modeling methods include grid-based methods and C-space methods [7,8]. This study adopts the grid-based method for urban flight environment modeling due to its simplicity and ease of implementation.

To validate the proposed algorithm's effectiveness, MATLAB is used to generate grid maps simulating urban 2D environments for the simulation. These maps include both static and mobile obstacles. The advantages of MATLAB for path planning simulation include its ability to create highly adaptable 2D maps and straightforward visualization of research outcomes. Figure 1 illustrates the grid map used in this study.

2.2 Optimized A-star

The traditional A-star algorithm requires longer search times in complex, large-scale areas. It calculates numerous node paths, consumes significant memory, and uses heuristic functions to find obstacle-avoidance paths in static maps [9]. However, it struggles to adapt to the dynamic and complex urban environment. During planning, the generated paths may have insufficient clearance from obstacles, reducing safety. In contrast, the Artificial Potential Field (APF) method assumes UAVs move under the combined forces of target attraction and obstacle repulsion. This approach produces smooth paths, is simple to implement, and serves as a novel obstacle-avoidance method for path planning.

This study combines the A-star algorithm with the APF method to create a hybrid obstacle-avoidance function. The A-star algorithm addresses the APF method's shortcomings in avoiding large obstacles [10]. The APF algorithm compensates for the A-star algorithm's inability to evade dynamic obstacles in real-time environments. By adjusting paths instantly based on current potential field conditions, the hybrid method reduces the search range required for pathfinding, generates smoother paths, enhances obstacle-avoidance precision, and reacts to moving obstacles.

To improve UAV safety, this paper uses the A-star algorithm to plan the global path. When obstacles are detected, the map is grid-divided to identify the obstacle-avoidance start and end nodes. The APF algorithm then plans a local detour route. After obstacle avoidance, the UAV continues path planning using the APF method. This cycle repeats until the target point is reached. The improved algorithm workflow is shown in Figure 2.

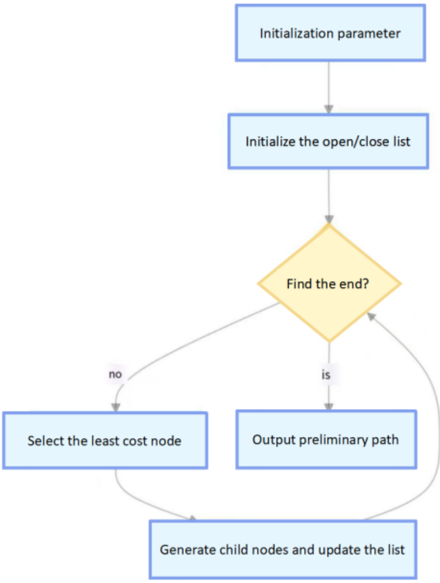

Fig. 2. Algorithm Workflow

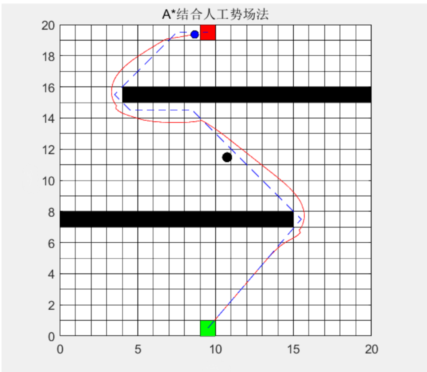

Fig. 3. Examples of routes, points and obstacles

2.2.1 Improvement of the Repulsion Field: the enhanced repulsion field not only considers the repulsive force from obstacles but also incorporates the influence of UAV velocity on repulsion. Collision avoidance is further achieved by calculating the velocity potential field repulsion. Assume the UAV's current coordinates are $X = (x, y)$, the obstacle's coordinates are $X_0 = (x_0, y_0)$, the danger distance is p, the obstacle is defined as $d = |X - X_0|$.

2.2.2 Calculation of the Repulsive Force F: when the distance d between the UAV and the obstacle is greater than or equal to the danger distance ρ, the UAV is unaffected by the repulsion field, and the repulsive force *F* is 0.

When $d < \rho$, the repulsive force *F* consists of two components：

A repulsive force directed from the obstacle to the UAV.

A repulsive force directed from the UAV to the target point.

$$\boldsymbol{F} = \begin{cases} \mathbf{0}, \boldsymbol{d} \geq \boldsymbol{\rho} \\ \boldsymbol{k}(\frac{\boldsymbol{d}^2}{2}) + \mathbf{0.5}\boldsymbol{k}(\frac{1}{\boldsymbol{d}} - \frac{1}{\boldsymbol{\rho}})^2, \boldsymbol{d} < \boldsymbol{\rho} \end{cases} \quad (1)$$

d Represents the Euclidean distance between the UAV's current position and the obstacle.

F1 Represents the repulsive force directed from the obstacle to the UAV.

F2 Represents the repulsive force directed from the UAV to the target point.

f(d) is a distance function that defines how the repulsive force varies with distance. *f(d)=1/d* （Inverse distance function）

When the distance *d* is less than ρ, the repulsive force decreases with the square of the distance.

2.2.3 Improvement of the Attraction Field Algorithm: assume the UAV’s current coordinates are *X= (x, y),* the target point coordinates are X:(), the attraction coefficient is k, and the distance between the UAV and the obstacle is *d* =| *X* - *Xo*|, where *X* = *(x0, y0)* represents the obstacle’s coordinates. Here,ρ denotes the danger distance between the UAV and the obstacle.

The formula for calculating the attraction field *U(X)* is as follows:

$$\boldsymbol{U(x)} = \frac{\boldsymbol{k(X-X_t)^2}}{\mathbf{2}} \quad (2)$$

(X-Xt) represents the vector difference between the UAV’s current position and the target point.K is the attraction coefficient, which adjusts the strength of the attraction field. $(X\text{-}Xt)^2$ denotes the squared norm of the vector difference, representing the squared distance between the UAV and the target point.

In path planning, the UAV’s movement direction is determined by the resultant force of attraction and repulsion. The direction of the resultant force dictates the UAV’s trajectory to avoid obstacles and move toward the target. The strength and direction of the attraction and repulsion fields may interact, influencing the UAV’s final path. The resultant force formula is:

$$\boldsymbol{F_t} = \begin{cases} \boldsymbol{k}\frac{(\boldsymbol{X}-\boldsymbol{X_t})^2}{2}, \boldsymbol{d} \geq \boldsymbol{\rho} \\ \boldsymbol{k}\frac{(\boldsymbol{X}-\boldsymbol{X_t})^2}{2} + \boldsymbol{k}\frac{\boldsymbol{d}^2}{2} + \mathbf{0.5}\boldsymbol{k}(\frac{1}{\boldsymbol{d}} - \frac{1}{\boldsymbol{\rho}})^2, \boldsymbol{d} < \boldsymbol{\rho} \end{cases} \tag{3}$$

3 Results

3.1 Validation of Path Planning Effectiveness

This study conducted simulation experiments using MATLAB R2020b on a computer with a Windows 10 operating system and 8GB RAM. A 2D spatial map of 200m × 200m was defined, containing two obstacles of non-negligible size. The Artificial Potential Field (APF) method was configured with an attraction coefficient of 5, a danger distance of 6m, and a UAV operating speed of 4m·s^{-1}. Both the A-star algorithm and the proposed algorithm were used to plan flight paths for the UAV from coordinate point (1, 1) to (20, 20) in the Oxy coordinate system, as shown on Figure 3.

The improved algorithm's flight path is demonstrated as follows: The UAV starts from the initial point (10, 1). First, the A-star algorithm performs global path planning to generate a preliminary route from the start to the target. The UAV then follows this path. When approaching an obstacle near point (14, 6), the algorithm switches to the APF method for local path optimization and obstacle avoidance. At this stage, the UAV utilizes the blue obstacle-avoidance path generated by the APF method to bypass the obstacle and navigate to point (15, 9). After reaching this point, the UAV continues combining Astar algorithm-based path planning until approaching the next obstacle near point (4, 14). At point (4, 14), the UAV again employs the APF method for local path optimization, avoiding the obstacle and moving to point (4, 17). Finally, guided by the A-star algorithm, the UAV follows the optimized path to reach the final target point (10, 20). When optimizing the A algorithm using the Artificial Potential Field (APF) algorithm in MATLAB, potential fields around obstacles are set to guide the search path away from obstacles. The figure shows the optimized path:

(1) Red squares represent the target point.

(2) Green squares indicate the starting point.

(3) Blue dots denote nodes in the A-star algorithm's search process.

(4) Black squares represent obstacles.

Table 1. Comparison of Minimum Distances to Obstacles in UAV Paths Using Different Algorithms (Unit: grid)

Algorithm	A-star Algorithm	Improved Algorithm
Start Point(10,1)	1.000	1.581

End Point(10,20)		
Start Point(1, 1) End Point(10, 20)	1.000	1.581
Start Point(1,1) End Point(15, 20)	0.707	1.000
Start Point(1, 1) End Point(20,20)	1.000	1.581
Start Point(15, 1) End Point(10,20)	0.707	1.000

Table 2. Comparison of Total Flight Path Lengths Using Different Algorithms for UAVs (Unit: grid)

Algorithm	A-star Algorithm	Improved Algorithm
Start Point(10,1) End Point(10,20)	23.677	23.3
Start Point(1, 1) End Point(10, 20)	22.735	22
Start Point(1,1) End Point(15, 20)	27.179	26.8
Start Point(1, 1) End Point(20,20)	29.250	28.3
Start Point(15, 1) End Point(10,20)	22.243	21.7

Dashed lines illustrate the direction of the potential fields.

With a safety distance set to 0.6, Table 1 demonstrates that, under varying start and end points in the same map, the shortest distances between the improved algorithm and obstacles—calculated using the Euclidean formula—exceed 0.6, meeting the safety distance criteria. These distances are also smaller than the shortest distances between the A-star algorithm's paths and obstacles. While ensuring safety, the improved algorithm achieves superior local path planning for obstacle avoidance.

Additionally, by comparing the total path lengths of UAV flight paths using the two algorithms across five groups, the A algorithm's total path length is slightly longer than that of the improved algorithm.* This indicates that the optimized algorithm demonstrates potential for higher efficiency and energy savings in global route planning compared to the traditional A-star algorithm, as shown in Table 2.

3.2 Validation of Path Planning Effectiveness

Blue lines represent the A algorithm, and red lines represent the optimized algorithm. The algorithms plan paths through segmented planning. In the right figure, black dots denote mobile obstacles. As shown in Figure 4. Example of avoiding moving obstacles, in the left figure, red squares mark nodes in the current path planning phase.

The traditional A-star algorithm's planned path overlaps with obstacles (visible in the figures), posing collision risks for the UAV. However, the optimized algorithm dynamically reacts to mobile obstacles, avoiding collisions. The improved algorithm generates smoother paths that maintain a safe distance from obstacles, enhancing safety. The total path length of the improved algorithm increases slightly, which aligns with expected results due to safety prioritization.

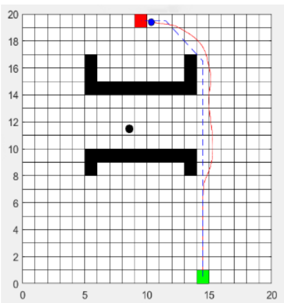
(a)

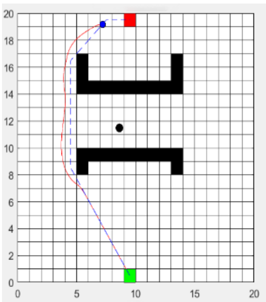
(b)

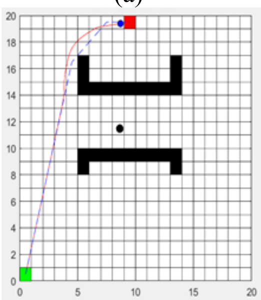
(c)

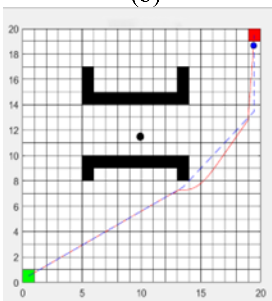
(d)

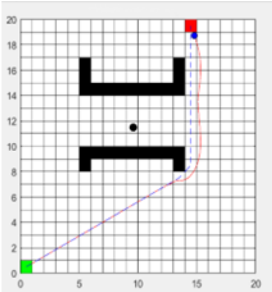

(e)

Fig. 4. Algorithm validation results based on different maps. (a)~(e) representing different maps.

4 Conclusion

This study addresses the limitations of the A-star algorithm in avoiding dynamic obstacles and maintaining safe distances near turning zones by integrating the Artificial Potential Field (APF) method. Simulation experiments in MATLAB validate the algorithm’s capability to dynamically evade obstacles in real time. Results show that the improved algorithm reduces path length by approximately 8% compared to the original A-star algorithm, while increasing the minimum distance between obstacles by about 50%. Simulations confirm that the optimized paths successfully avoid obstacles, with the A-star algorithm’s nodes (blue dots) maintaining safe distances from obstacles. This demonstrates that the A-star algorithm, augmented by APF, can effectively plan collision-free paths. Furthermore, the method ensures high efficiency and reliability in path planning due to minimal interference. The optimized algorithm does not excessively disrupt the A-star algorithm’s natural search process but provides guidance when necessary, achieving superior path planning in complex environments.

These improvements significantly enhance path safety, effectively reducing accident risks. This advancement holds great significance for UAV applications in urban low-altitude logistics and contributes to the development of low-altitude economies in cities. The hybrid path planning method, combining A-star and APF, first generates a coarse path using A-star and then optimizes it with APF to avoid dynamic obstacles and produce smoother trajectories. This approach improves both safety and efficiency. While the current method achieves core functionalities—dynamic obstacle handling and path smoothing—future research could refine potential field functions or integrate machine learning techniques to further enhance performance.

Authors Contribution

Jiaqi Song is responsible for Abstract, Keywords, Introduction, Literature review 1, References and Conclusion. Rongjun Zhou is responsible for Literature review 2 and 3.

All the authors contributed equally and their names were listed in alphabetical order.

References

1. Fleureau J., Galvane Q., Tariolle F.L., Guillotel P. 'Generic Drone Control Platform for Autonomous Capture of Cinema Scenes; Proceedings of the 2nd Workshop on Micro Aerial Vehicle Networks', Systems, and Applications for Civilian Usel; Singapore. 26 June 2016; New York, NY, USA: ACM; 2016. pp. 35–40.
2. Quadt, T., Lindelauf, R., Voskuijl, M, Monsuur, H., & Ule, B. 'Dealing with multiple optimization objectives for uav path planning in hostile environments: a literature review'. DRONES, 2024, 8(12), 769.
3. Wu, J., Wang, H., Li, N, Yao, P., Huang, Y., & Yang, H. (2017). 'Path planning for solar-powered uav in urban environment'. NEUROCOMPUTING, S0925231217316880.
4. Chamoso P, González-Briones A, Rivas A, Bueno De Mata F, Corchado JM. 'The Use of Drones in Spain: Towards a Platform for Controlling UAVs in Urban Environments'. Sensors (Basel). 2018 May 3;18(5):1416.
5. Huang X. 'The small-drone revolution is coming—scientists need to ensure it will be safe'. Nature, 2025, 637(8044): 29-30.
6. Wu E, Sun Y, Huang J, et al. 'Multi UAV cluster control method based on virtual core in improved artificial potential field'. IEEE Access, 2020, 8: 131647-131661.
7. Feng J, Zhang J, Zhang G, et al. 'UAV dynamic path planning based on obstacle position prediction in an unknown environment'. IEEE Access, 2021, 9: 154679-154691.
8. Ait Saadi A, Soukane A, Meraihi Y, et al. 'UAV path planning using optimization approaches: A survey. Archives of Computational Methods in Engineering', 2022, 29(6): 4233-4284.
9. Du Y, Zhang X, Nie Z. 'A real-time collision avoidance strategy in dynamic airspace based on dynamic artificial potential field algorithm'. IEEE Access, 2019, 7: 169469-169479.
10. Rao J, Xiang C, Xi J, et al. 'Path planning for dual UAVs cooperative suspension transport based on artificial potential field-A-star algorithm'. Knowledge-Based Systems, 2023, 277: 110797.